THE ASTROPHYSICAL JOURNAL, 430:L89–L92, 1994 August 1

ON DETERMINING THE SPECTRUM OF PRIMORDIAL INHOMOGENEITY FROM THE *COBE*[1] DMR SKY MAPS: RESULTS OF TWO-YEAR DATA ANALYSIS

K. M. GÓRSKI,[2,3,4] G. HINSHAW,[5] A. J. BANDAY,[2] C. L. BENNETT,[6] E. L. WRIGHT,[7]
A. KOGUT,[5] G. F. SMOOT,[8] AND P. LUBIN[9]
Received 1994 March 29; accepted 1994 May 11

ABSTRACT

A new technique of Fourier analysis on a cut sky has been applied to the two-year *COBE* DMR 53 and 90 GHz sky maps. The Bayesian power spectrum estimation results are consistent with the Harrison-Zel'dovich $n = 1$ model. The maximum likelihood estimates of the usual parameters defining the power spectrum of primordial perturbations are $n = 1.22$ (1.02) and $Q_{\rm rms-PS} = 17$ (20) μK including (excluding) the quadrupole. A spectral-index-independent normalization is naturally expressed for the two-year maps in terms of the multipole amplitude $a_9 = 8.2$ (8.3) μK (to $\sim 12\ \sigma$ significance). The marginal likelihood function on n obtained by integration with respect to a_9 renders $n = 1.17 \pm 0.31$ (0.96 ± 0.36).

Subject headings: cosmic microwave background — cosmology: observations

1. INTRODUCTION

The determination of the power spectrum of primordial inhomogeneities and their consistency with the predictions of inflation are critical issues in contemporary cosmology. Standard inflationary scenarios imply a power-law spectrum $P(k) \propto k^n$, with $n \simeq 1$ on the scales probed in the *COBE* DMR sky maps. Previous attempts to determine the primordial power spectrum from the DMR anisotropy data (using the first year data: Smoot et al. 1992; Wright et al. 1992; Adams et al. 1992; Scaramella & Vittorio 1993; Seljak & Bertschinger 1993; Smoot et al. 1994; Bond 1994; using the two year data: Bennett et al. 1994; Wright et al. 1994a) found both relatively steep spectra and sensitivity to the inclusion or exclusion of the quadrupole in their results. Most methods have employed approximate statistical techniques and have relied on Monte Carlo techniques to assess and/or calibrate the final results.

In this *Letter* the *COBE* DMR two-year 53 and 90 GHz data are analyzed to determine the primordial power spectrum using the method described in Górski (1994). Specifically, the sky maps are Fourier decomposed in the basis of orthonormal functions on the Galaxy-cut sky to yield a set of harmonic mode coefficients, which are linear in the pixel temperatures. These are then used in a maximum likelihood analysis to infer the parameters of the theoretical anisotropy models. The merits of the present method are (1) harmonic mode coupling is explicitly accounted for by construction of the orthonormal functions on the Galaxy-cut sky, (2) since the harmonic modes have a Gaussian probability distribution an *exact* likelihood function for the model parameters can be employed, (3) the monopole and dipole components, which are physically irrelevant for the power spectrum estimation, are algebraically excluded, and (4) the technique permits a simultaneous analysis of different frequency maps taking full advantage of both the auto- and cross-correlation information in the data.

In this analysis we Fourier decompose the two-year DMR sky maps over the spectral range up to $\ell = 30$, where the DMR beam response has fallen to ~ 0.2 (Wright et al. 1994b), and the multipole amplitude is entirely noise dominated. No attempt is made to model and subtract formally the diffuse high-latitude Galactic emission, which is predominantly quadrupolar in nature. Therefore, in what follows, the power spectrum parameters are derived for two cases: one in which data spanning the multipole range $\ell \in [2, 30]$ are used, and the other in which the quadrupole ($\ell = 2$) mode is excluded.

Hereafter, bold upper case letters denote matrices; bold lower case letters denote vectors; and p is a pixel label. Specific equations from Górski (1994) will be referred to by "G" immediately followed by the equation number.

2. DATA

Each individual DMR sky map is a collection of 6144 pixelized measurements of temperature perturbations, $\Delta(p)$, comprising cosmological, receiver noise, Galactic, and systematic signals. The instrument noise is characterized by the number of observations per pixel, and an rms noise per observation, σ_0 (derived from Table 1 of Bennett et al. 1994). In order to limit the effects of Galactic emission on the power spectrum determination, a $|b| = 20°$ Galaxy cut is imposed on the maps, reducing the number of pixels to 4016 in each map. Systematic effects have been strongly limited (Bennett et al. 1994) and are neglected in this analysis, as are the weak high-latitude Galactic signals. The 53 and 90 GHz two year cut-sky maps are analyzed in this work. We form weighted average maps at each frequency by combining the individual A and B channels as follows:

$$\Delta_{53} = 0.578\Delta_{53A} + 0.422\Delta_{53B}\ ,$$
$$\Delta_{90} = 0.366\Delta_{90A} + 0.634\Delta_{90B}\ , \qquad (1)$$

[1] The National Aeronautics and Space Administration/Goddard Space Flight Center (NASA/GSFC) is responsible for the design, development, and operation of the *Cosmic Background Explorer* (*COBE*). Scientific guidance is provided by the *COBE* Science Working Group. GSFC is also responsible for the development of the analysis software and for the production of the mission data sets.

[2] Universities Space Research Association, NASA/Goddard Space Flight Center, Code 685.3, Greenbelt, MD 20771.
[3] On leave from Warsaw University Observatory, Aleje Ujazdowskie 4, 00-478 Warszawa, Poland.
[4] E-mail: gorski@stars.gsfc.nasa.gov.
[5] Hughes STX Corporation, 4400 Forbes Blvd., Lanham, MD 20706.
[6] NASA Goddard Space Flight Center, Code 685, Greenbelt, MD 20771.
[7] UCLA Astronomy Department, Los Angeles, CA 90024-1562.
[8] LBL, SSL, & CfPA, Bldg 50-351, University of California, Berkeley, CA 94720.
[9] UCSB Physics Department, Santa Barbara, CA 93106.

where all temperatures are in thermodynamic units. These weights were chosen to minimize the average noise variance per pixel in the combined maps. Fourier analysis of the cut-sky maps is performed in the 961-dimensional linear space, spanned by the orthonormal functions ψ constructed by Górski (1994). The harmonic coefficients of a map in the ψ basis are given by (see G8 and G3)

$$\Delta(p)|_{p\in\{\text{cut sky}\}} = c^T\cdot\psi(p)\,, \quad \text{where } c = \langle\Delta\psi\rangle_{\{\text{cut sky}\}}\,. \qquad (2)$$

The data vector for joint analysis of the 53 and 90 GHz data was formed according to $c^T_{53\oplus 90} = (c^T_{53}, c^T_{90})$.

3. LIKELIHOOD ANALYSIS

The covariance matrices, $\mathbf{C} = \mathbf{C}_{\rm CMB} + \mathbf{C}_N$, of the harmonic amplitudes, $c = c_{\rm CMB} + c_N$, specify the Gaussian probability distribution (eq. [G15]) of the receiver-noise-contaminated theoretical CMB anisotropy signal. The power-spectrum-dependent matrix $\mathbf{C}_{\rm CMB}$ can be parameterized by two quantities, $Q_{\rm rms-PS}$ and n (see eqs. [G10] and [G11]).

The receiver noise is modeled as a spatially uncorrelated Gaussian random process with a frequency-dependent variance per pixel $\sigma^2(p) = \langle\Delta^2_N(p)\rangle_{\{\text{noise ensemble}\}} = \sigma_0^2/N(p)$. Equation (G13) was used to obtain the Fourier space noise correlation matrices $\mathbf{C}_N$. The resulting rms noise amplitude per harmonic mode is 4.8 μK for the 53 GHz data, and 7.8 μK for the 90 GHz data. These values are important for an a priori assessment of the sensitivity of DMR to the anisotropy predicted by a particular cosmology.

Having established an appropriate mathematical representation of the data, specifically the Fourier amplitude vector $c_{53\oplus 90}$, the anisotropy correlation matrix $\mathbf{C}_{\rm CMB}$, and the noise correlation matrices $\mathbf{C}_{N53}$ and $\mathbf{C}_{N90}$, we can perform a Bayesian likelihood analysis to determine the power spectrum parameters $Q_{\rm rms-PS}$ and n. The necessary ingredients for a proper Bayesian statistical analysis (e.g., Berger 1980) are the likelihood function of data given a model, $P(\text{data}\,|\,\text{model})$, and the prior distribution of the model, $\pi(\text{model})$. These then define the posterior distribution for the model given the data, $P(\text{model}\,|\,\text{data}) \propto \pi(\text{model}) \times P(\text{data}\,|\,\text{model})$. We evaluate the likelihood function for the *COBE* DMR data, $c_{53\oplus 90}$, given a model parameterized by $Q_{\rm rms-PS}$ and n (see eqs. [G15] and [G16]), either including or excluding the quadrupole anisotropy (which involves correlation matrices of dimension 1914 or 1904, respectively).

Figure 1 shows two views of the likelihood function evaluated with the quadrupole anisotropy included; the no quadrupole case yields qualitatively similar contours. This likelihood function is confined to a very narrow and steep ridge in the parameter space conveniently defined by the multipole amplitude $a_9(Q_{\rm rms-PS}, n) \simeq 8$ μK (see eq. [G11]). Clearly any prior $\pi(Q_{\rm rms-PS}, n)$ that is slowly varying near the peak of the likelihood will not significantly affect the inference on $Q_{\rm rms-PS}$ and n. We have tested the sensitivity of the derived maximum likelihood parameter values and credible intervals to some specific assumptions about π. The following prior distributions were considered: (1) $\pi = \text{const}$, (2) $\pi \propto 1/(1+n)$, (3) $\pi \propto (1+n)$, (4) $\pi \propto 1/Q_{\rm rms-PS}$, (5) $\pi \propto Q_{\rm rms-PS}$, (6) $\pi \propto 1/(1+n)/Q_{\rm rms-PS}$, and (7) $\pi \propto (1+n)Q_{\rm rms-PS}$. As expected the results are robust to ~ 1 μK in $Q_{\rm rms-PS}$, and ~ 0.1 in n. Hence, in the following we adopt a constant prior distribution.

Figure 2 shows the 68%, 95%, and 99.7% contours for the posterior distributions of $Q_{\rm rms-PS}$ and n evaluated with and without the quadrupole anisotropy. Exclusion of the quadrupole from the analysis results in considerable elongation of the likelihood contours toward low-n and high-$Q_{\rm rms-PS}$ values. This is the region of the parameter space seriously constrained by the inclusion of the relatively low observed quadrupole (Bennett et al. 1994). The following approximate formulae describe the location of the ridge of the posterior distributions: $Q_{\rm rms-PS}(n) = (39+2n)\exp(-0.73n)$, or $Q_{\rm rms-PS}(n) = (40+2n)\exp(-0.74n)$, with or without quadrupole, respectively (accurate to ~ 0.5 μK within the plotted contours).

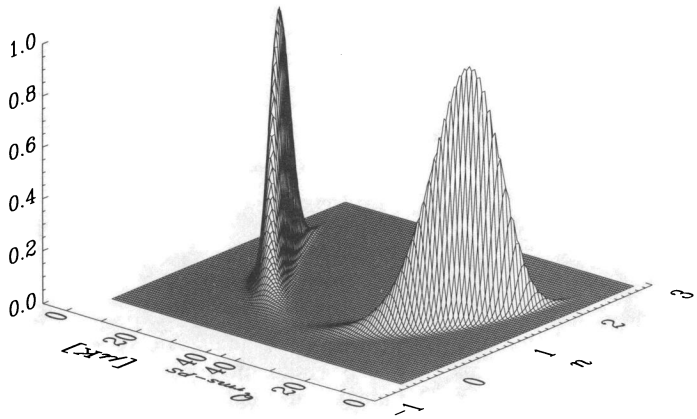

FIG. 1.—Two views of the likelihood function, $P(Q_{\rm rms-PS}, n)$ derived in a simultaneous analysis of the 53 and 90 GHz *COBE*-DMR two-year data including harmonic amplitudes from the range $\ell \in [2, 30]$.

Inference on a subset of parameters among those that naturally characterize a given problem is usually arranged by marginalization, or integration of the posterior distribution with respect to all of the parameters except for those of interest. In the case here, the parameter of special interest is the spectral index n, for which the marginal likelihood density is obtained by integration, $p(n) \propto \int dQ_{\rm rms-PS}\, P(Q_{\rm rms-PS}, n\,|\,c_{53\oplus 90})$. An alternative method for the construction of a posterior distribution on n alone involves the projection of $P(Q_{\rm rms-PS}, n\,|\,c_{53\oplus 90})$ onto the (P, n) plane, that is, treating $Q_{\rm rms-PS}$ as a "nuisance" parameter. Such marginal and projected likelihoods on n are shown in Figure 3. It should be noted that the maximum likelihood values for n derived from the marginal distributions are

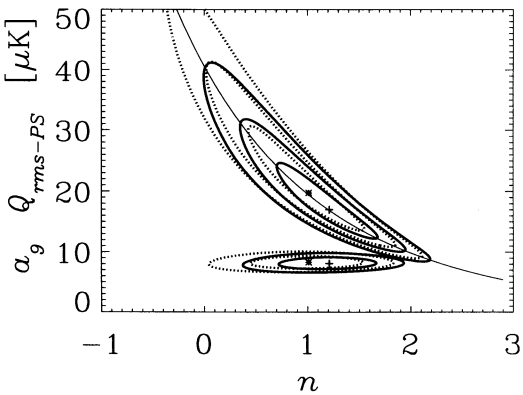

FIG. 2.—Contour plots and the loci of the maxima for the likelihood functions. The upper set of contours represents the 68%, 95%, and 99.7% levels for the function $P(Q_{\rm rms-PS}, n)$. The thin solid line defined by $a_9(Q_{\rm rms-PS}, n) = \text{const}$ very closely follows the ridge of the likelihoods. The lower set of contours represents the 68%, and 95% levels for the function $P(a_9, n)$. Solid lines and plus signs represent the results of the analysis including the quadrupole. Dotted lines and asterisks show the no quadrupole case.

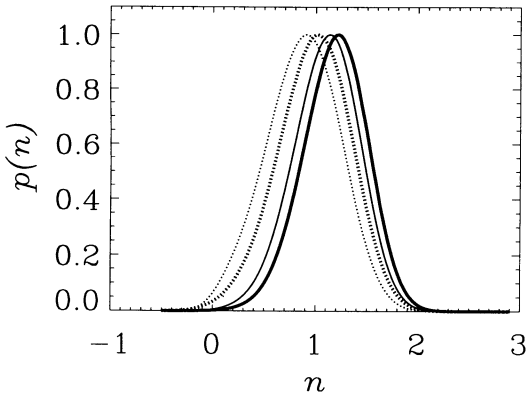

FIG. 3.—Likelihood densities on the spectral index n derived from $P(Q_{\rm rms-PS}, n)$ (arbitrary normalization). The solid curves include the quadrupole in the analysis; the dotted curves exclude the quadrupole. The marginal likelihood densities, $p(n) \propto \int dQ_{\rm rms-PS} P(Q_{\rm rms-PS}, n)$ are shown in the lighter type. The projected likelihood densities derived on treating $Q_{\rm rms-PS}$ as a nuisance parameter are shown in the heavier type. These are identical to both marginal and projected likelihood densities on n derived from $P(a_9, n | c_{53\oplus 90})$.

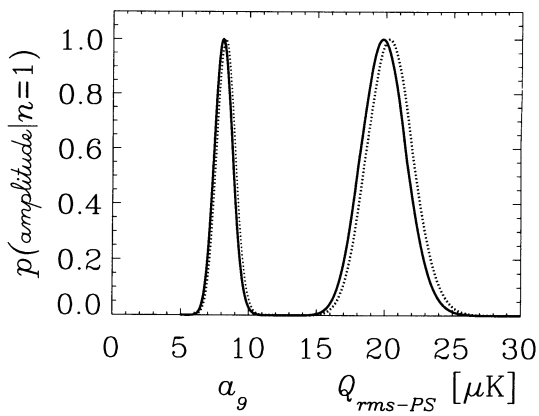

FIG. 4.—The $n = 1$-conditional likelihood densities (arbitrary normalization) for a_9 and $Q_{\rm rms-PS}$. The solid curves include the quadrupole, the dotted curves are the no quadrupole case.

lower than those derived from the two-dimensional posterior distribution. This is a consequence of the specific shape of $P(Q_{\rm rms-PS}, n | c_{53\oplus 90})$, which implies that $Q_{\rm rms-PS}$ and n are not independent. The projected likelihood is maximized at the same value of n as in the two-dimensional analysis by construction.

As a result of the choice of a_9 instead of $Q_{\rm rms-PS}$ as a parameter to normalize the power spectrum the posterior distributions (shown in Fig. 2) are now defined in terms of two nearly independent variables. The derivation of marginal and projected distributions on n now renders practically indistinguishable results, which are those shown in Figure 3 as the projected distributions derived under the $Q_{\rm rms-PS}$ and n parameterization.

The conditional likelihood density on a_9 and $Q_{\rm rms-PS}$ for $n = 1$ (the Harrison-Zel'dovich spectrum) are shown in Figure 4.

Numbers relevant to the above discussion are presented in Table 1.

4. DISCUSSION

Miscellaneous issues pertaining to the proper assessment of our results include (1) noise model uncertainties, (2) the question of biases in parameter inference, and (3) comparison to other attempts at determination of the power spectrum from the two-year data set.

The method of power spectrum determination presented in this *Letter* requires an adequate description of the statistical properties of noise in the sky maps. In order to test the correctness of construction of the Gaussian noise ensemble, we have evaluated the Fourier components of the cut-sky two-year difference maps, c_{A-B}, at both frequencies, and the a priori

TABLE 1

DERIVED PARAMETERS FROM THE LIKELIHOOD ANALYSIS OF *COBE* DMR TWO-YEAR SKY MAPS

A. $(Q_{\rm rms-PS}, n)$ PLANE

PARAMETERS	INCLUDING QUADRUPOLE $Q_{\rm rms-PS}$ (μK)	INCLUDING QUADRUPOLE n	EXCLUDING QUADRUPOLE $Q_{\rm rms-PS}$ (μK)	EXCLUDING QUADRUPOLE n
Maximum likelihood values	17.0	1.22	20.0	1.02
68% credible interval	[12.2, 24.6]	[0.70, 1.68]	[13.5, 30.5]	[0.43, 1.55]
95% credible interval	[10.0, 31.8]	[0.35, 1.95]	[10.6, 41.5]	[0.02, 1.85]
Marginal likelihood on n	1.10 ± 0.32		0.87 ± 0.36	
Conditional likelihood on $Q^{n=1}_{\rm rms-PS}$	19.9 ± 1.6		20.4 ± 1.7	

B. (a_9, n) PLANE

PARAMETERS	INCLUDING QUADRUPOLE a_9 (μK)	INCLUDING QUADRUPOLE n	EXCLUDING QUADRUPOLE a_9 (μK)	EXCLUDING QUADRUPOLE n
Maximum likelihood values	8.1	1.22	8.3	1.01
68% credible interval	[7.2, 9.1]	[0.72, 1.67]	[7.3, 9.4]	[0.45, 1.53]
95% credible interval	[6.6, 9.9]	[0.37, 1.93]	[6.7, 10.1]	[0.04, 1.83]
Marginal likelihood on n	1.17 ± 0.31		0.96 ± 0.36	
Projected likelihood on n	1.19 ± 0.31		0.98 ± 0.36	
Conditional likelihood on $a^{n=1}_9$	8.1 ± 0.7		8.3 ± 0.7	
Marginal likelihood on a_9	8.2 ± 0.7		8.3 ± 0.7	

difference map noise covariance matrices (see eq. [G13]), $\mathbf{C}_{N(A-B)}$. The reduced χ^2, defined as $\boldsymbol{c}_{A-B}^T \cdot \mathbf{C}_{N(A-B)} \cdot \boldsymbol{c}_{A-B}/N$ where $N = 957$, is 0.93 at 53 GHz and 1.06 at 90 GHz. This validates the a priori noise model constructed using the flight rms noise values and the actual patterns of the number of observations per pixel. Nevertheless, the noise rms per observation, σ_0, is only known to an accuracy of $\sim 1\%$. The possibility of a mismatch between the assumed and the actual noise levels can perturb the spectral index and amplitude estimation. Specifically, an underestimate of the noise leaves some small-scale power which the likelihood method translates into a steeper spectrum than required by the true sky anisotropy, and vice versa. If σ_0 is adjusted by $\sim 1\%$, the maximum likelihood values for $Q_{\mathrm{rms-PS}}$ and n are shifted by ~ 0.5 μK and ~ 0.04, respectively, insignificant amounts when compared to the overall uncertainty in the inferred spectrum.

In principle, maximum likelihood estimates of nonlinear model parameters are only asymptotically unbiased. In order to test whether any biases exist in this analysis, we performed various Monte Carlo simulations of noisy random skies drawn from an ensemble of fixed $Q_{\mathrm{rms-PS}}$ and n and with the noise properties of the two-year 53 GHz maps. We have simulated the observed maps both in Fourier space limited to $\ell_{\mathrm{max}} = 30$ and in pixel space, that is, with no limit imposed on the ℓ-range of the noise component of the maps. In both the Fourier and pixel space simulations no statistically significant bias in the simulated sample-averaged estimates of the parameters $Q_{\mathrm{rms-PS}}$ and n was detected when the quadrupole was either included or excluded. (Thus, Fourier analysis limited to $\ell_{\mathrm{max}} = 30$ is sufficient for the inference of the sky anisotropy power spectrum.) A subensemble of simulations with suppressed quadrupole amplitudes was also considered. Here, only those sky map realizations with an $\ell = 2$ power amplitude in the ψ basis, $\sum_{i=5}^{9} c_i^2$, no greater than that observed in the two year 53 GHz data were included. In this case, a general bias was observed to lower $Q_{\mathrm{rms-PS}}$ and higher n ($\delta Q \sim -3$ μK and $\delta n \sim 0.3$). Given that the observed sky quadrupole is low with respect to our inferred ensemble-averaged value of $Q_{\mathrm{rms-PS}} \simeq 20$ μK for $n = 1$, this affords a plausible explanation for the small $\delta n \sim 0.2$ difference between spectral slopes inferred from the sky maps with or without the quadrupole (see Table 1).

By choosing $\ell_{\mathrm{max}} = 30$ we have analyzed the *COBE* DMR two-year sky maps over a spectral range larger than previously implemented. Other methods are inherently less sensitive to the high-ℓ information content of the data either as a consequence of additional binning or smoothing of the data (e.g., Bennett et al. 1994; Smoot et al. 1994), or by construction (e.g., Wright et al. 1994a, where originally $\ell_{\mathrm{max}} = 19$ was adopted). We have tested the effect of using the restricted spectral range $\ell \in [3, 19]$ as a direct comparison with Wright et al. (1994a). The maximum likelihood estimates in this case are $Q_{\mathrm{rms-PS}} = 17.8$ μK, and $n = 1.22$. The steepening of the resulting spectrum is driven by the relatively high amplitude of several modes within $\ell \in [14, 19]$ in the 53 GHz sum map. In addition, we find that the power in the corresponding bin of the 53 GHz $(A-B)$ difference map falls below the a priori noise model, thus Wright et al. determine a still higher power in their quadratic power spectrum estimator. With the inclusion of $\ell \geq 20$ modes the effect of this excess is more effectively constrained and attributed to noise. It should be noted that in the final revision of their paper, Wright et al. (1994a) have extended their derivation of the power spectrum over the full $\ell \in [3, 30]$ range considered in this *Letter*. This renders a less steep power spectrum estimate, $n = 1.25^{+0.4}_{-0.45}$, than in the original version of their work, and is now in better agreement with our no quadrupole results. A more detailed comparison of the application of different methods of power spectrum inference is deferred to a future paper.

In summary, the new, statistically unbiased technique of power spectrum determination described in Górski (1994) has been implemented for the *COBE* DMR 53 and 90 GHz two-year sky maps. The results are consistent with the Harrison-Zel'dovich $n = 1$ spectrum favored by inflationary models. If this is indeed the case, then the two year *COBE* DMR data provide a ~ 12 σ significant detection, $Q_{\mathrm{rms-PS}} \simeq 20$ μK (or $a_9 \simeq 8$ μK *independent* of n), for the amplitude of the spectrum of primordial inhomogeneity.

We gratefully acknowledge the efforts of those contributing to the *COBE* DMR. *COBE* is supported by the Office of Space Sciences of NASA Headquarters.

REFERENCES

Adams, F. C., Bond, J. R., Freese, K., Frieman, J. A., & Olinto, A. V. 1992, Phys. Rev. D, D47, 426
Bennett, C. L., et al. 1994, ApJ, submitted
Berger, J. O. 1980, Statistical Decision Theory and Bayesian Analysis (New York: Springer)
Bond, J. R. 1994, CITA-94-5, astro-ph/9402043
Górski, K. M. 1994, ApJ, 430, L85
Scaramella, R., & Vittorio, N. 1993, MNRAS, 263, L17
Seljak, U., & Bertschinger, E. 1993, ApJ, 417, L9
Smoot, G. F., et al. 1992, ApJ, 396, L1
———. 1994, ApJ, in press
Wright, E. L., et al. 1992, ApJ, 396, L13
———. 1994a, ApJ, in press
———. 1994b, ApJ, 420, 1